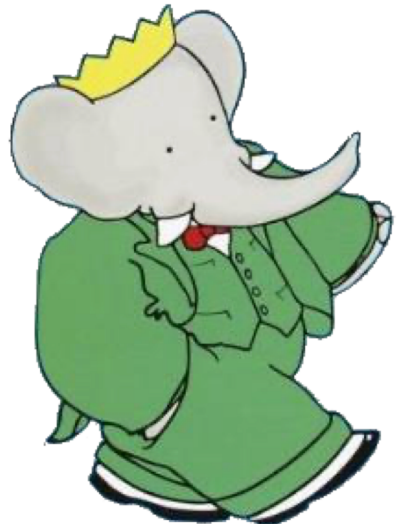


Recent *BaBar* results on measurement of exclusive hadronic cross sections



Evgeny Solodov for BaBar Collaboration

BudkerINP, Novosibirsk, Russia

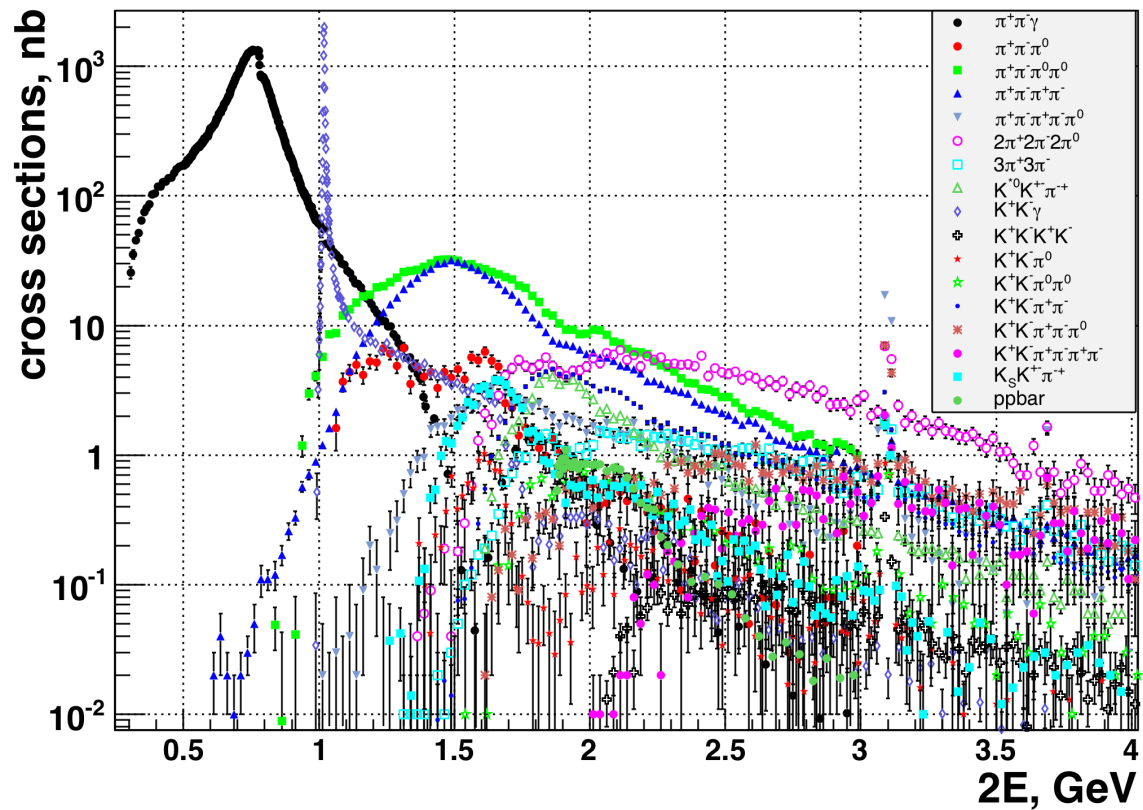
June 29, 2021

Outline

- Recently completed (published) analyses
 - $e^+e^- \rightarrow 2(\pi^+\pi^-)\pi^0\pi^0\pi^0(\eta)$ – reported at ICHEP2020, published Phys. Rev. D 103 (2021) 092001
 - $e^+e^- \rightarrow \pi^+\pi^-\pi^0\pi^0\pi^0\pi^0(\eta)$ – reported at ICHEP2020, preliminary, at last stage review - soon
- Analyses in progress
 - $e^+e^- \rightarrow \pi^+\pi^-\pi^0$ new analysis, x5 more data
 - $e^+e^- \rightarrow \pi^+\pi^-$ new analysis, x7 more data, new method
 - $e^+e^- \rightarrow 2K3\pi$ new analysis
- Conclusion

BaBar low energy hadron cross sections

- BaBar has developed the ISR tools and is continuing an intensive program for low energy e+e- cross section study for more than 15 years.
- At the moment BaBar has presented most complete set of exclusive cross sections at low c.m. energies
- Uncertainties vary from 0.5-2% for 2h, 3-5% for 3-4hadrons and 7-15% for multi-hadron states.
- BaBar data have very important role in HVP calculations, somewhere dominate.
- BaBar still plans to improve already published data and plans to present new measurements.



BaBar ISR measurements (March 2021)

$2(\pi^+\pi^-)\pi^0\pi^0\pi^0$, $2(\pi^+\pi^-)\pi^0\pi^0\eta$	Phys. Rev. D 103 (2021) 092001
$\pi^+\pi^-\pi^0\pi^0\pi^0$, $\pi^+\pi^-\pi^0\pi^0\eta$	Phys. Rev. D 98 (2018) 112015
$\pi^+\pi^-\pi^0\pi^0$	Phys. Rev. D 96 (2017) 092009
$\pi^+\pi^-\eta$	Phys. Rev. D 97 (2018) 052007
$K_S^0 K_L^0 \pi^0$, $K_S^0 K_L^0 \eta$, and $K_S^0 K_L^0 \pi^0\pi^0$	Phys. Rev. D 95 (2017) 052001
$K_S^0 K^+ \pi^-\pi^0$, $K_S^0 K^+ \pi^-\eta$	Phys. Rev. D 95 (2017) 092005
K^+K^-	γ undet. Phys. Rev. D 92 (2015) 072008
$K_S^0 K_L^0$, $K_S^0 K_L^0 \pi^+\pi^-$, $K_S^0 K_S^0 \pi^+\pi^-$, $K_S^0 K_S^0 K^+K^-$	γ undet. Phys. Rev. D 89 (2014) 092002
$\bar{p}p$	γ undet. Phys. Rev. D 88 (2013) 072009
$\bar{p}p$	NLO Phys. Rev. D 87 (2013) 092005
K^+K^-	NLO Phys. Rev. D 88 (2013) 032013
$\pi^+\pi^-$	NLO Phys. Rev. Lett. 103 (2009) 231801
$2(\pi^+\pi^-)$	Phys. Rev. D 85 (2012) 112009
$K^+K^-\pi^+\pi^-$, $K^+K^-\pi^0\pi^0$, $K^+K^-K^+K^-$	Phys. Rev. D 86 (2012) 012008
$K^+K^-\eta$, $K^+K^-\pi^0$, $K^0K^\pm\pi^\mp$	Phys. Rev. D 77 (2008) 092002
$2(\pi^+\pi^-)\pi^0$, $2(\pi^+\pi^-)\eta$, $K^+K^-\pi^+\pi^-\pi^0$, $K^+K^-\pi^+\pi^-\eta$	Phys. Rev. D 76 (2007) 092005
$\Lambda\bar{\Lambda}$, $\Lambda\Sigma^0$, $\Sigma^0\Sigma^0$	Phys. Rev. D 76 (2007) 092006
$3(\pi^+\pi^-)$, $2(\pi^+\pi^-\pi^0)$, $K^+K^-2(\pi^+\pi^-)$	Phys. Rev. D 73 (2006) 052003
$\pi^+\pi^-\pi^0$	Phys. Rev. D 70 (2004) 072004

Magenta: First measurements,

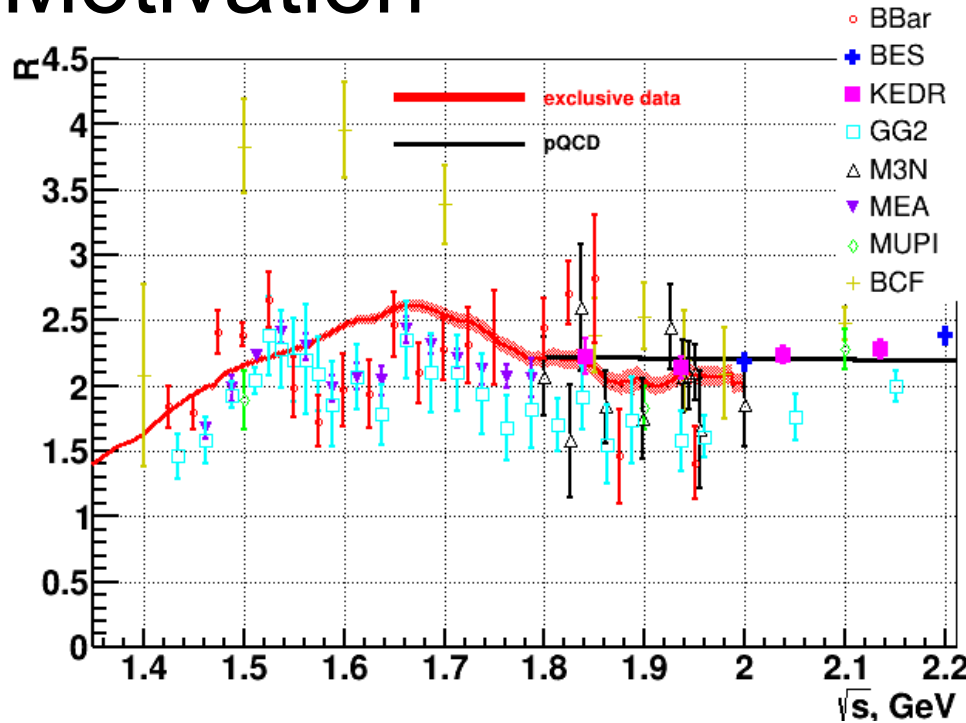
Green: $454 - 469 \text{ fb}^{-1}$,

Cyan: 232 fb^{-1} ,

Blue: 89 fb^{-1}

Superseded results omitted

Motivation



Because of large, highly granulated calorimeter BaBar has advantage for study of the multi-photon reactions over detectors at VEPP2000 (SND and CMD-3) even effective integrated luminosity is already lower.

Currently, the sum of exclusive cross sections near 2.0 GeV shows a systematic deviation from the QCD predictions.

BABAR, SND and CMD-3 measurements of previously unmeasured processes, e.g. $e^+e^- \rightarrow \pi^+\pi^-\pi^0\pi^0\pi^0\pi^0$, $\pi^+\pi^-\pi^+\pi^-\pi^0\pi^0\pi^0$, $K_S K^+ \pi^- \pi^0\pi^0$, $K^- K^+ \pi^0\pi^0\pi^0$, ... may help to understand if this discrepancy is real.

$e^+e^- \rightarrow 2(\pi^+\pi^-)\pi^0\pi^0\pi^0(\eta)$ and $\pi^+\pi^-\pi^0\pi^0\pi^0\pi^0(\eta)$ at c.m. energies from threshold to 4.5 GeV using ISR

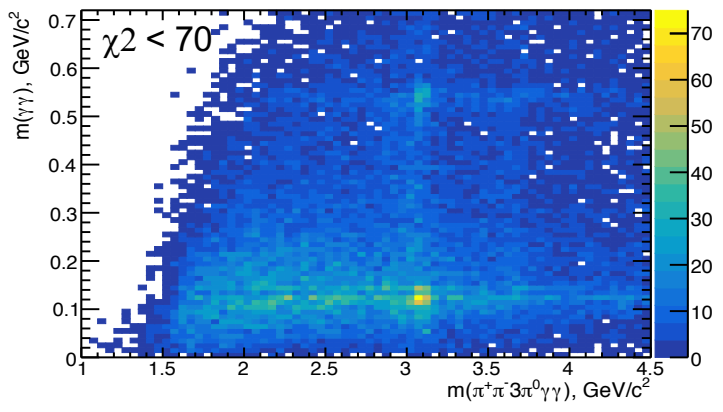
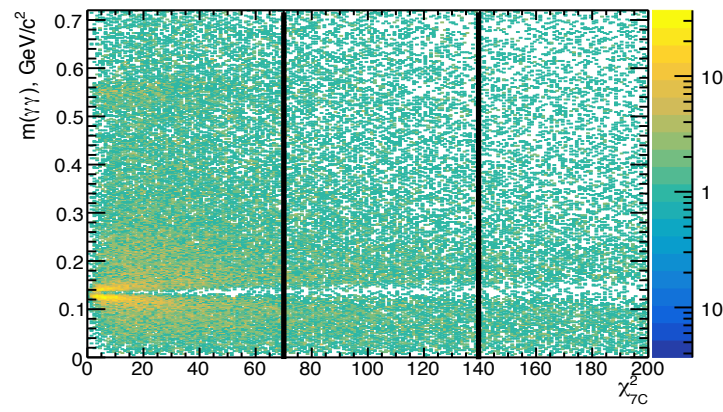
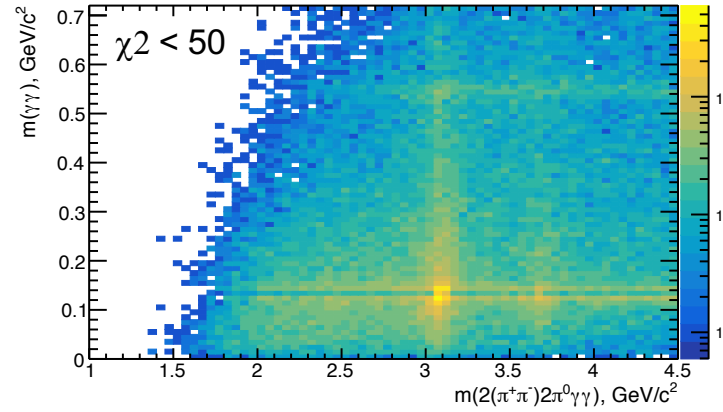
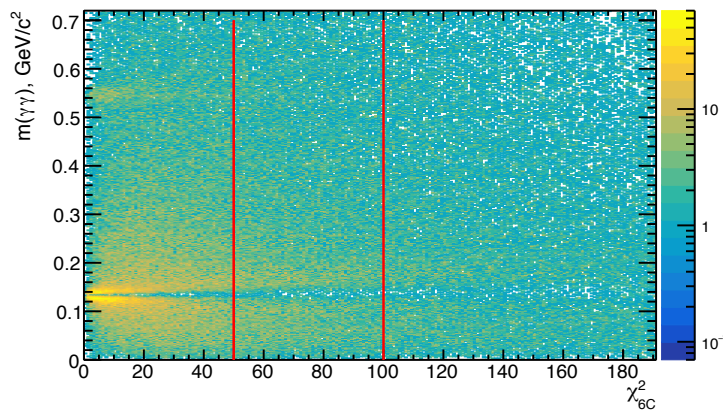
Analyses are based on tools developed for the $e^+e^- \rightarrow \pi^+\pi^-\pi^0\pi^0\pi^0$ - published in
Phys.Rev. D98 (2018) no.11, 112015 - two charged or one π^0 are added to the procedure

- 469 fb⁻¹ of BaBar data
- ~200k MC simulation for $e^+e^- \rightarrow 2\pi^0\eta\gamma$ (PS, $\omega\pi^0\eta\gamma$)
- ~500k MC simulation for $e^+e^- \rightarrow \omega\eta\gamma$
- MC includes all radiative processes
- Background processes (from MC):
 $e^+e^- \rightarrow \tau^+\tau^-$
 $e^+e^- \rightarrow qq$ ($q = u,d,s,c$) - major background is from $e^+e^- \rightarrow 4\pi^0, 2\pi^0\pi^0$
 $e^+e^- \rightarrow 3\pi\gamma, 4\pi\gamma, 5\pi\gamma, 6\pi\gamma, 4\pi^0\gamma(!) - \omega\eta$ final state

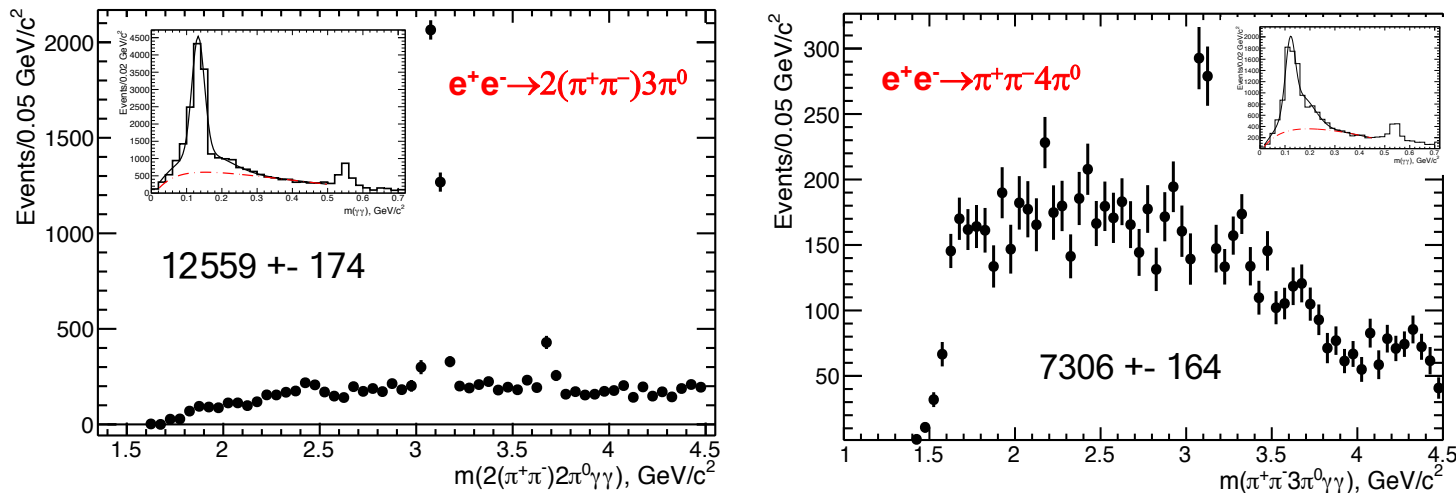
Analysis procedure (without details):

- Select events with 4(2) charged tracks and 7(9) or more photons (up to 25 sometimes)
- Take most energetic photon as ISR
- For each independent set of 6(8) photons test all combinations of 3(4) $\gamma\gamma$ pairs with ± 35 MeV windows around π^0 mass.
- Perform 6C (7C) fit in $4\pi^0\gamma\gamma_{\text{ISR}}$ ($2\pi^0\gamma\gamma_{\text{ISR}}$) hypothesis with π^0 mass constrain for two (three) best pairs, NO constrain on mass for 3rd (4th) $\gamma\gamma$ pair.
- Look for best χ^2 , trying all pairs to be 3rd or 4th

Experimental distributions for 3rd (4th) $\gamma\gamma$ pair



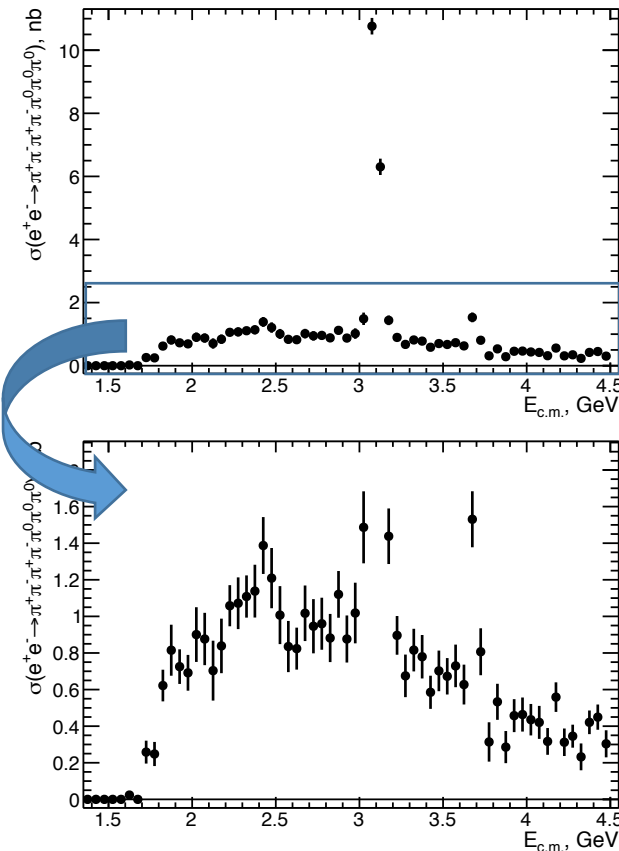
Fit of π^0 signal in data



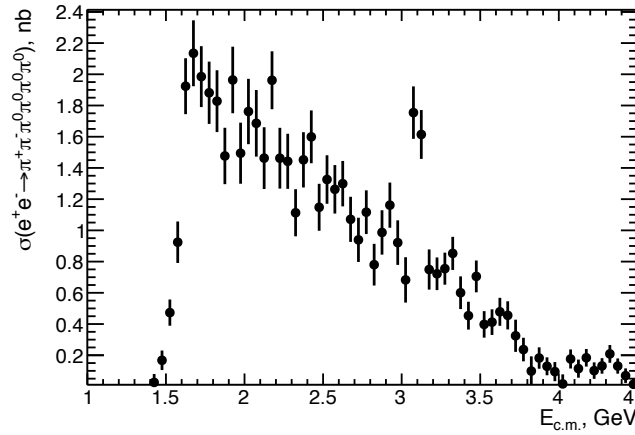
Fit in every 0.05 GeV, using π^0 shape from simulation after background subtraction from control region. Remaining background - a polynomial function.

Cross sections

$e^+e^- \rightarrow 2(\pi^+\pi^-)\pi^0\pi^0\pi^0$



$e^+e^- \rightarrow \pi^+\pi^-\pi^0\pi^0\pi^0\pi^0$



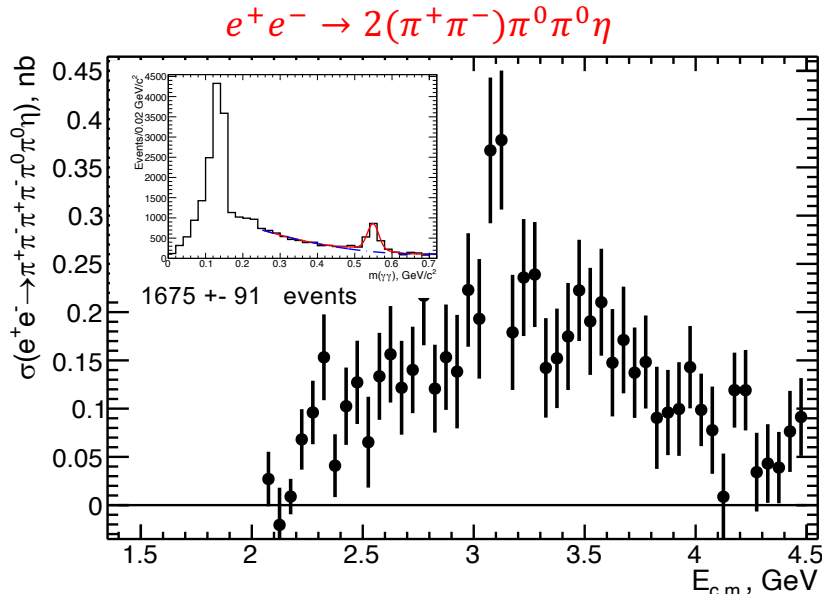
Corrections and systematic uncertainties:

Fit procedure	--	5-7%
Tracking efficiency	+4(2)	2%(1%)
Luminosity	--	1%
Efficiency(model + fits)	--	5%
χ^2 cut uncertainty	--	3%
π^0 efficiency	+9(12)	3%(4%)
Radiative corr.	--	1%
ISR photon eff.	+1.5	0.5%
Total	+14.5(15.5)	~10%

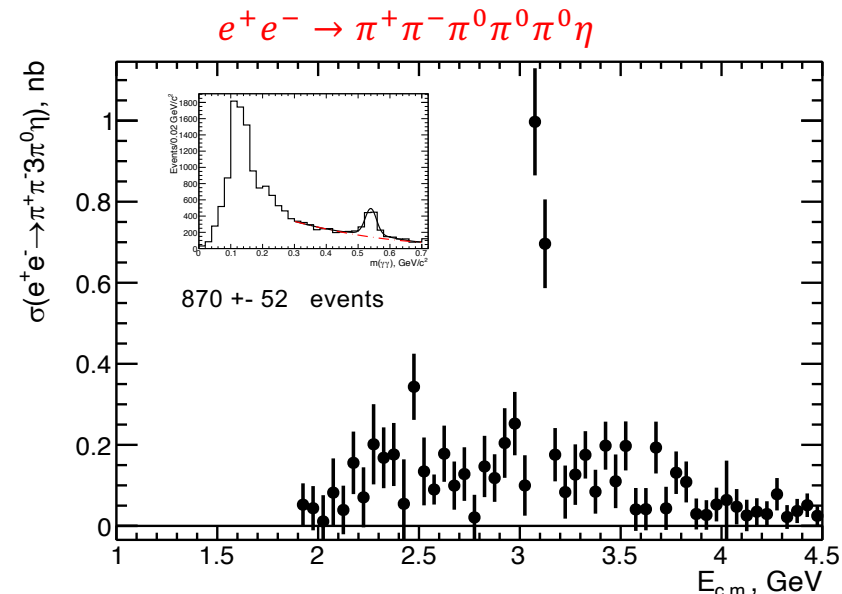
No other measurements

Similar fit of η signal

Using η shape as double Gaussian and flat background shape, we fit for every $0.05 \text{ GeV}/c^2$



Well above 2 GeV, events are normalized by efficiency and lumi for the cross section.

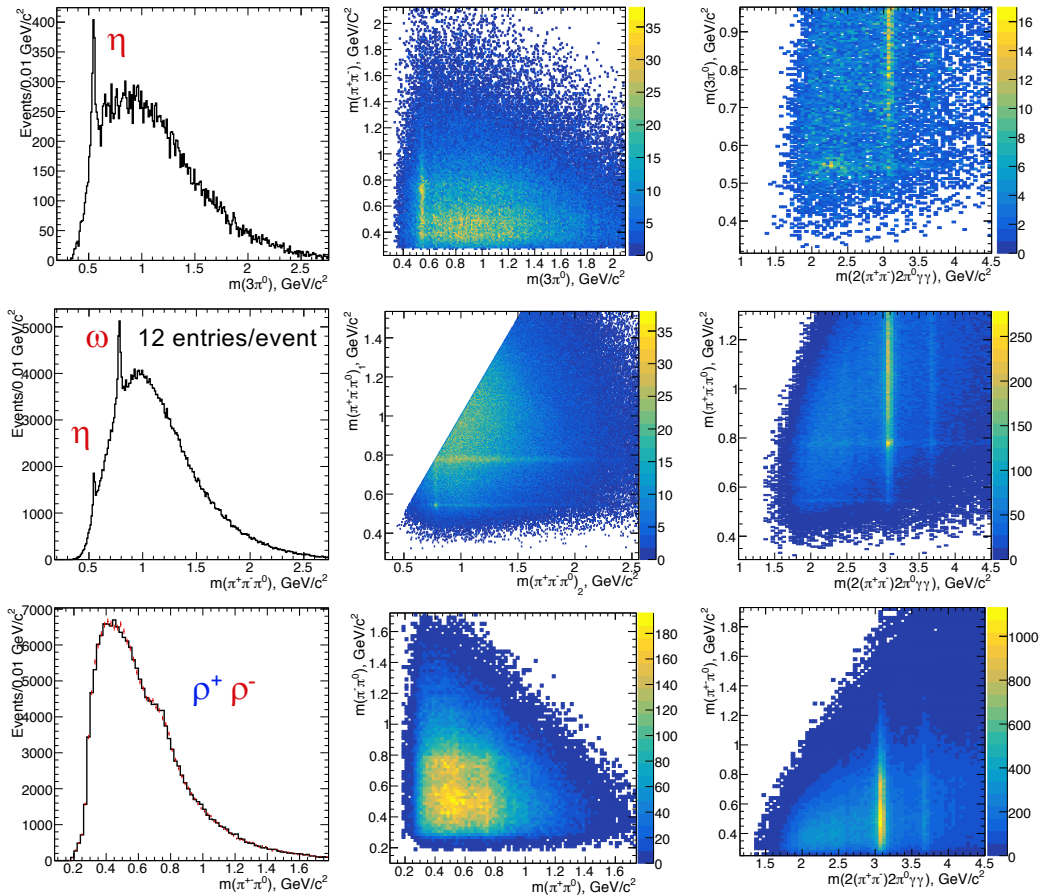


$\text{BR}(\eta \rightarrow \gamma\gamma)$ is taken into account

Well above 2 GeV – J/psi BR is large...

No other measurements

What we have inside of 7π ? $m(\gamma\gamma) < 0.3 \text{ GeV}/c^2$



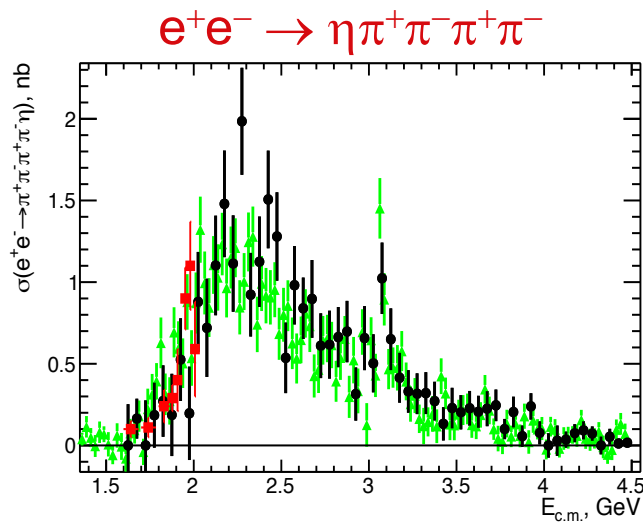
Dominates by

$$e^+e^- \rightarrow \eta\pi^+\pi^-\rho^0 (a_1\pi\eta)$$

$$e^+e^- \rightarrow \omega(\eta)\pi^+\pi^-\pi^0\pi^0, \\ \omega\eta\pi^0$$

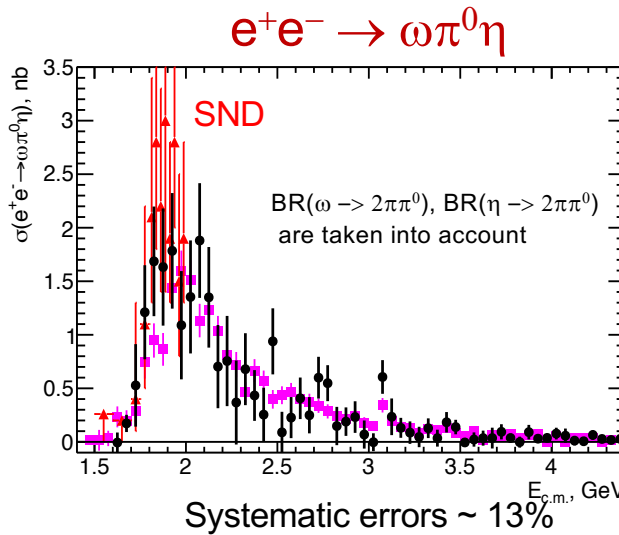
$$e^+e^- \rightarrow \rho^\pm 5\pi, (\rho^+\rho^- 3\pi)? \\ J/\psi \text{ production dominates}$$

Cross sections for intermediate states in $4\pi 3\pi^0$

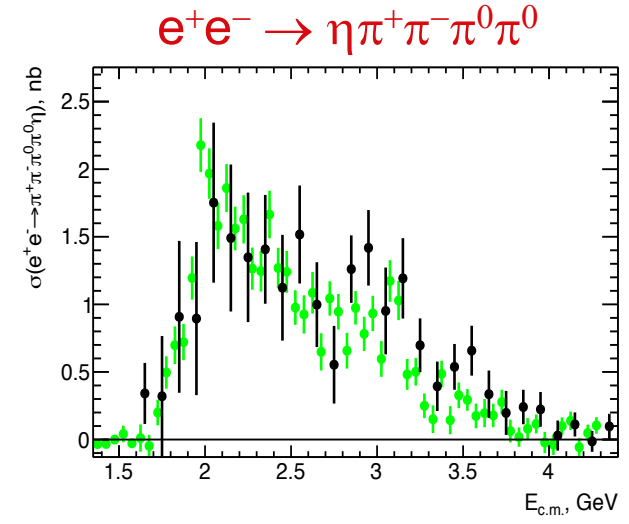


$BR(\eta \rightarrow 3\pi^0)$ is taken into account

BaBar $\eta \rightarrow \gamma\gamma$ ([Phys.Rev. D76 \(2007\) 092005](#))
CMD-3 $\eta \rightarrow \pi^+\pi^-\pi^0$ [Phys.Lett. B792 \(2019\) 419-423](#)



We are in agreement with the BaBar data for the $e^+e^- \rightarrow \omega\pi^0\eta(\eta \rightarrow \gamma\gamma)$ reaction [Phys.Rev. D98 \(2018\) no.11, 112015](#), and still are lower than SND measurement.

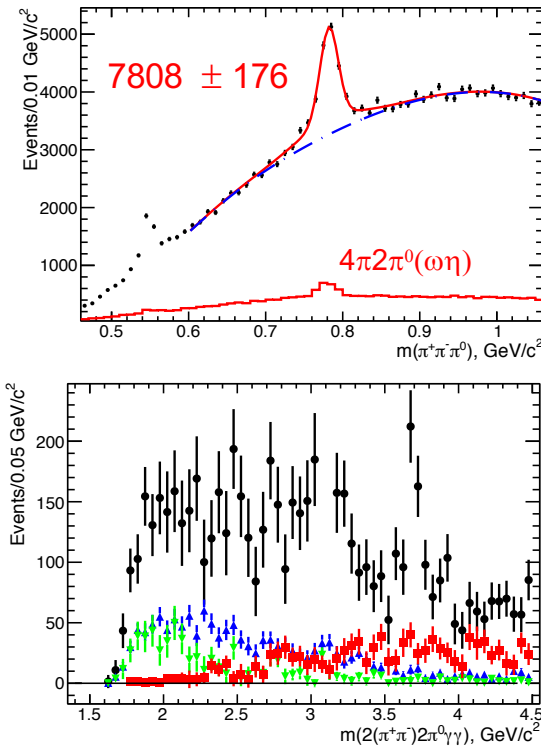


Cross section is shown for the 0.1 GeV intervals.

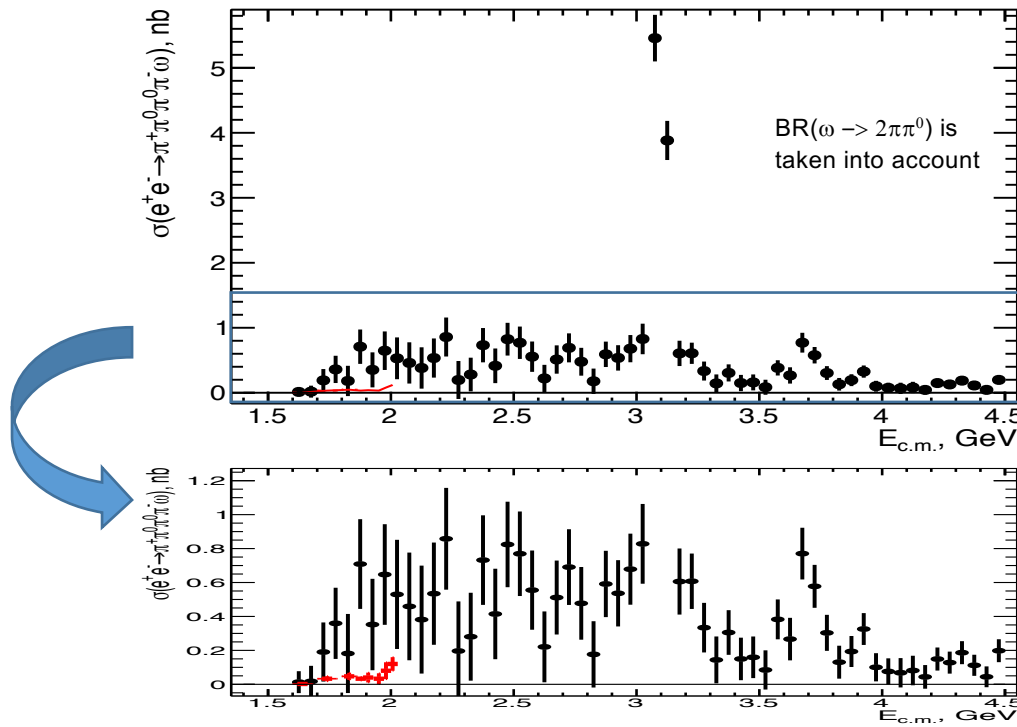
Reasonable agreement with our recent result for $\eta \rightarrow \gamma\gamma$ mode
[Phys.Rev. D98 \(2018\) no.11, 112015](#)

Good agreement with previously measured cross sections in different decay modes of ω, η

Cross section for $e^+e^- \rightarrow \omega \pi^+\pi^-\pi^0\pi^0$



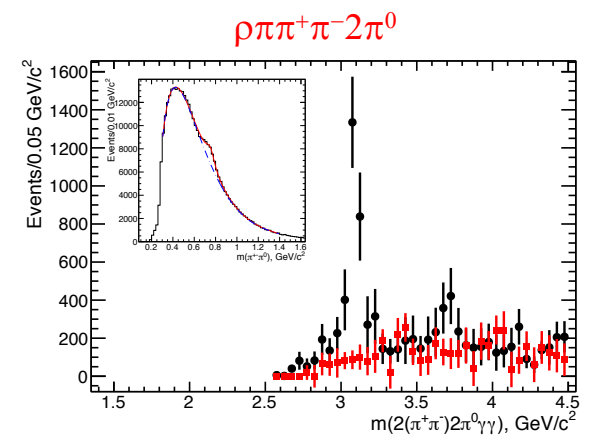
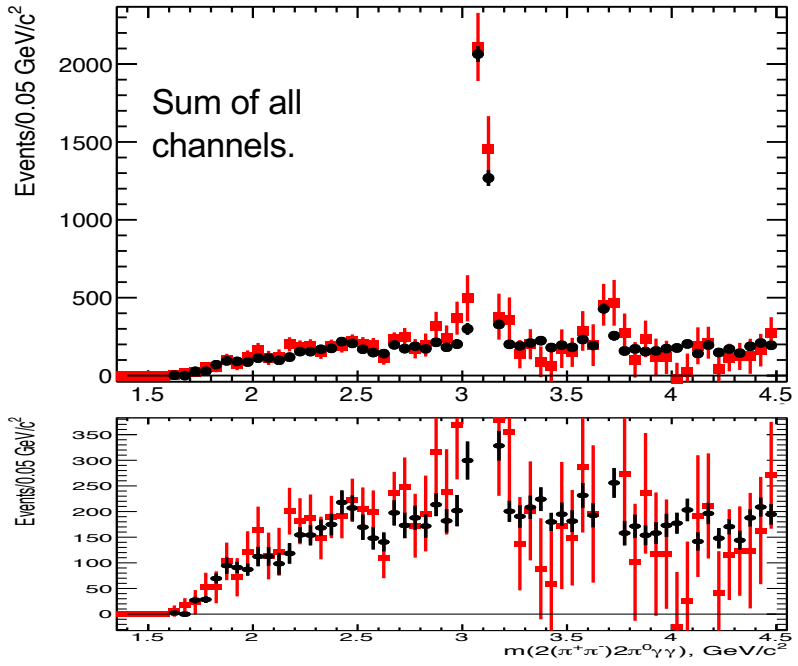
We subtract peaking background contribution from $4\pi 2\pi^0$, events from $\omega\pi^0\eta$ reaction, and uds



No other measurements

CMD-3 results are shown for the $e^+e^- \rightarrow \omega \pi^+\pi^-\pi^+\pi^-$ reaction
Phys.Lett. B792 (2019) 419-423

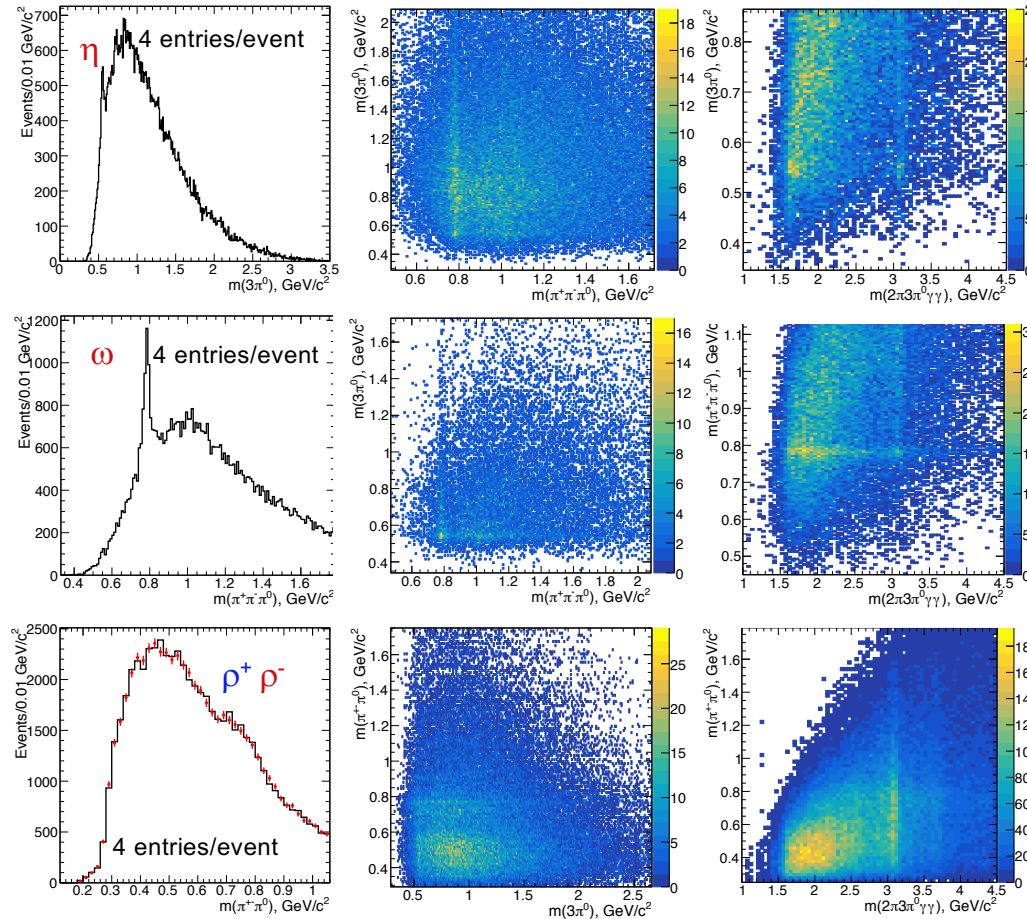
Contribution from different channels



ρ signal is scaled by
 $(2014+415)/2844 = 0.85$
to account for $\rho^+\rho^-$

The observed $4\pi 3\pi^0$ events are covered by the $\omega\pi^0\eta$, $\omega\pi^+\pi^-2\pi^0$, $\eta\pi^+\pi^-2\pi^0$, $\eta 2(\pi^+\pi^-)$ for < 3 GeV, and includes $\rho\pi\pi^+\pi^-2\pi^0$ channels for $>2.5-3$ GeV

What we have inside of 6π ?



$$|m(\gamma\gamma) - m\pi^0| < 0.1 \text{ GeV}/c^2$$

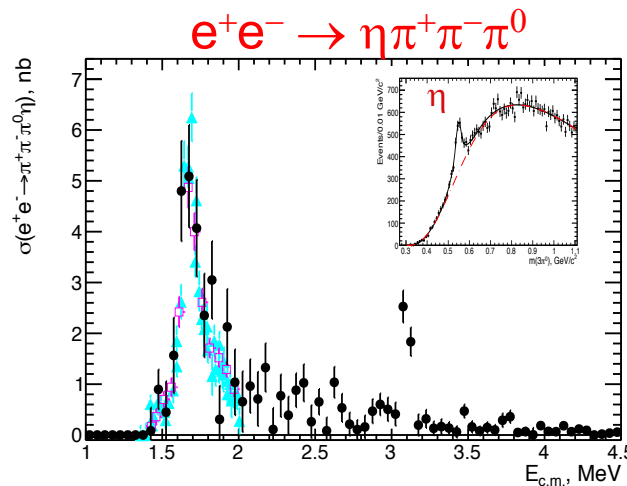
Dominates by

$$e^+e^- \rightarrow \eta\pi^+\pi^-\pi^0, \omega\eta$$

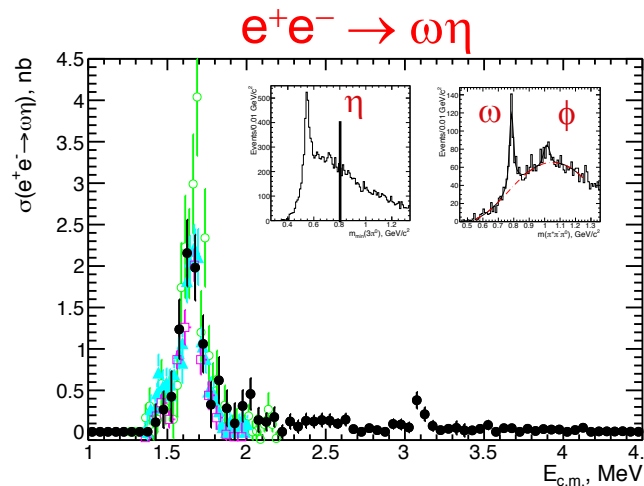
$$e^+e^- \rightarrow \omega(\phi)\pi^0\pi^0\pi^0, \\ \omega(\phi)\eta$$

$$e^+e^- \rightarrow \rho^\pm 4\pi, \\ \rho^\pm\pi^+\eta? \rho^\pm\rho^\mp 2\pi^0? \\ J/\psi \text{ production dominates}$$

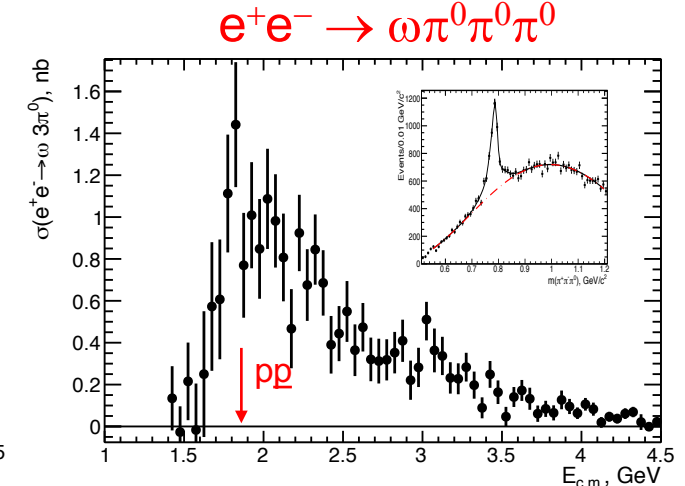
Cross sections for intermediate states in $2\pi 4\pi^0$



CMD-3 ([Phys.Lett. B773 \(2017\) 150-158](#))
 SND ([Phys.Rev. D99 \(2019\) no.11, 112004](#))
 have published this cross section for
 $\eta \rightarrow \gamma\gamma$ mode up to 2.0 GeV



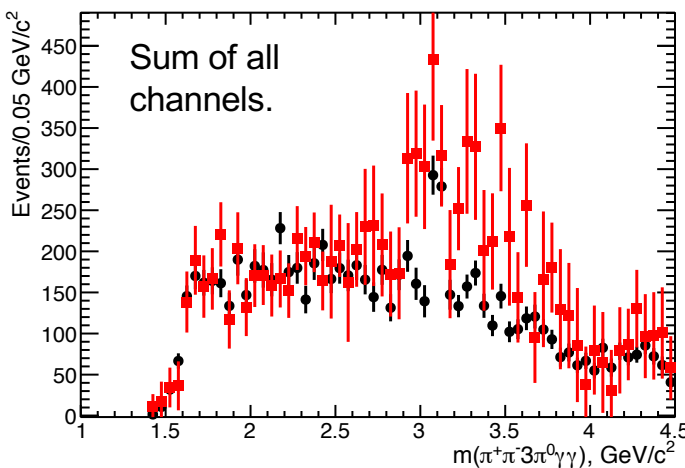
We are lower than the BaBar data for the
 $e^+e^- \rightarrow \omega\eta (\eta \rightarrow 2\pi\pi^0)$ reaction, and in
 agreement with SND and CMD-3
 measurements.



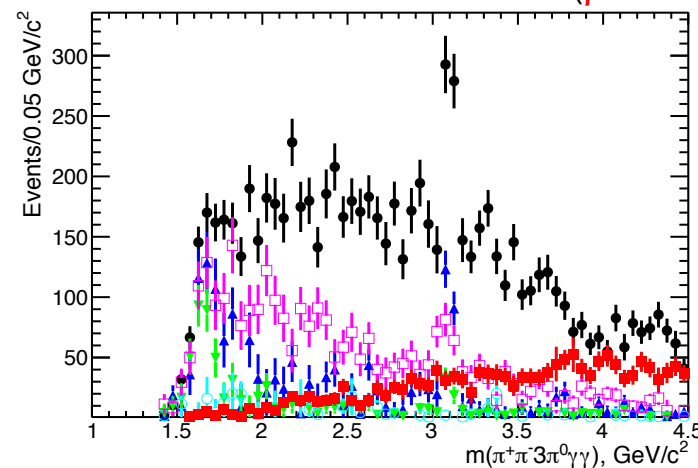
No other measurements

Good agreement with previously measured cross sections in different decay modes of ω, η

Contribution from different channels



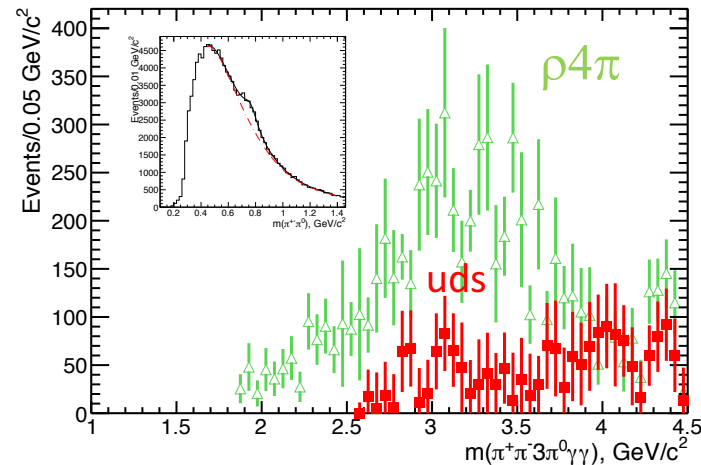
Contribution from selected intermediate states ($\rho 4\pi$ is not shown)



The observed $2\pi 4\pi^0$ events are covered by the $\pi^+\pi^-\pi^0\eta(\omega\eta)$, $\omega 3\pi^0$, $\rho\pi 3\pi^0$ for $< \sim 2.9 \text{ GeV}$, and probably some contribution from $\rho^+\rho^-2\pi^0$ channels for $2.9-4.0 \text{ GeV}$

29.06.2021

Solodov BaBar



17

J/ ψ region for $\pi^+\pi^-\pi^+\pi^-\pi^0\pi^0\pi^0$ and $\pi^+\pi^-\pi^0\pi^0\pi^0\pi^0$

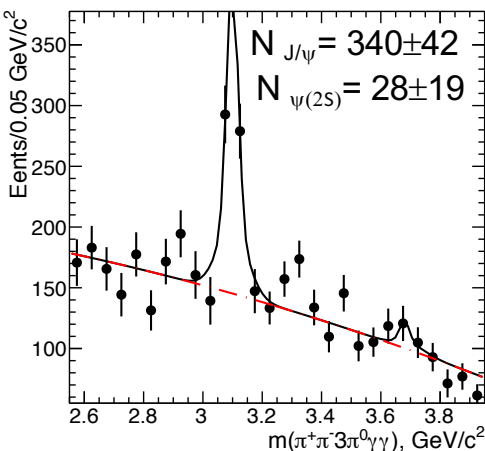
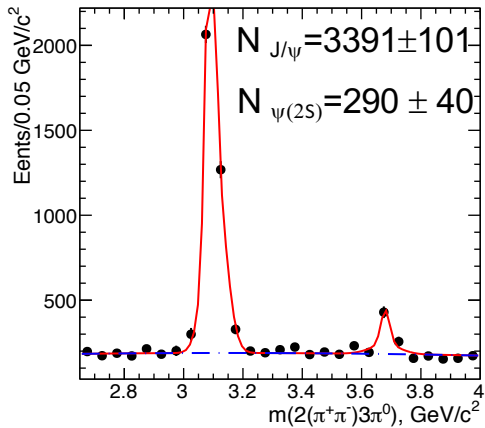


TABLE VIII: Summary of the J/ψ and $\psi(2S)$ branching fractions.

Measured Quantity	Measured Value (eV)	J/ψ or $\psi(2S)$ Branching Fraction (10 ⁻³) Calculated, this work	PDG [28]
$\Gamma_{ee}^{J/\psi} \cdot \mathcal{B}_{J/\psi \rightarrow \pi^+\pi^-\pi^+\pi^-\pi^0\pi^0\pi^0}$	$345.0 \pm 10.0 \pm 50.0$	$62.0 \pm 2.0 \pm 9.0$	no entry
$\Gamma_{ee}^{J/\psi} \cdot \mathcal{B}_{J/\psi \rightarrow \omega\pi^+\pi^-\pi^0\pi^0} \cdot \mathcal{B}_{\omega \rightarrow \pi^+\pi^-\pi^0}$	$165.0 \pm 9.0 \pm 25.0$	$33.0 \pm 2.0 \pm 5.0$	no entry
$\Gamma_{ee}^{J/\psi} \cdot \mathcal{B}_{J/\psi \rightarrow \eta\pi^+\pi^-\pi^0\pi^0} \cdot \mathcal{B}_{\eta \rightarrow \pi^+\pi^-\pi^0}$	$6.0 \pm 4.0 \pm 1.0$	$4.8 \pm 3.2 \pm 0.8$	2.3 ± 0.5
$\Gamma_{ee}^{J/\psi} \cdot \mathcal{B}_{J/\psi \rightarrow \pi^+\pi^-\pi^-\pi^-\eta} \cdot \mathcal{B}_{\eta \rightarrow \pi^0\pi^0\pi^0}$	$5.6 \pm 2.6 \pm 0.8$	$2.6 \pm 1.2 \pm 0.5$	2.26 ± 0.28
$\Gamma_{ee}^{J/\psi} \cdot \mathcal{B}_{J/\psi \rightarrow \rho^\pm\pi^\mp\pi^+\pi^-\pi^0\pi^0}$	$155.0 \pm 26.0 \pm 36.0$	$28.0 \pm 4.7 \pm 6.6$	no entry
$\Gamma_{ee}^{J/\psi} \cdot \mathcal{B}_{J/\psi \rightarrow \rho^+\rho^-\pi^+\pi^-\pi^0}$	$32.0 \pm 13.0 \pm 15.0$	$5.7 \pm 2.4 \pm 2.7$	no entry
$\Gamma_{ee}^{J/\psi} \cdot \mathcal{B}_{J/\psi \rightarrow \pi^+\pi^-\pi^-\pi^-\pi^0\eta} \cdot \mathcal{B}_{\eta \rightarrow \gamma\gamma}$	$9.1 \pm 2.6 \pm 1.4$	$4.2 \pm 1.2 \pm 0.6$	no entry
$\Gamma_{ee}^{\psi(2S)} \cdot \mathcal{B}_{\psi(2S) \rightarrow \pi^+\pi^-\pi^+\pi^-\pi^0\pi^0}$	$33.0 \pm 5.0 \pm 5.0$	$14.0 \pm 2.0 \pm 2.0$	no entry
$\Gamma_{ee}^{\psi(2S)} \cdot \mathcal{B}_{\psi(2S) \rightarrow J/\psi\pi^0\pi^0} \cdot \mathcal{B}_{J/\psi \rightarrow \pi^+\pi^-\pi^+\pi^-\pi^0}$	$14.8 \pm 2.6 \pm 2.2$	$34.7 \pm 6.1 \pm 5.2$	33.7 ± 2.6
$\Gamma_{ee}^{\psi(2S)} \cdot \mathcal{B}_{\psi(2S) \rightarrow J/\psi\pi^+\pi^-} \cdot \mathcal{B}_{J/\psi \rightarrow \pi^+\pi^-\pi^0\pi^0\pi^0}$	$19.2 \pm 4.5 \pm 3.2$	$23.8 \pm 5.6 \pm 3.6$	27.1 ± 2.9
$\Gamma_{ee}^{\psi(2S)} \cdot \mathcal{B}_{\psi(2S) \rightarrow \omega\pi^+\pi^-\pi^0\pi^0} \cdot \mathcal{B}_{\omega \rightarrow \pi^+\pi^-\pi^0}$	$18.0 \pm 4.0 \pm 3.0$	$8.7 \pm 1.9 \pm 1.5$	no entry
$\Gamma_{ee}^{\psi(2S)} \cdot \mathcal{B}_{\psi(2S) \rightarrow \pi^+\pi^-\pi^+\pi^-\pi^0\eta} \cdot \mathcal{B}_{\eta \rightarrow \gamma\gamma}$	<1.9 at 90% C.L.	<2.0 at 90% C.L.	no entry
$\Gamma_{ee}^{\psi(2S)} \cdot \mathcal{B}_{\psi(2S) \rightarrow \pi^+\pi^-\pi^+\pi^-\eta} \cdot \mathcal{B}_{\eta \rightarrow \pi^0\pi^0\pi^0}$	<2.3 at 90% C.L.	<2.4 at 90% C.L.	1.2 ± 0.6

The largest decay mode of J/ψ !!

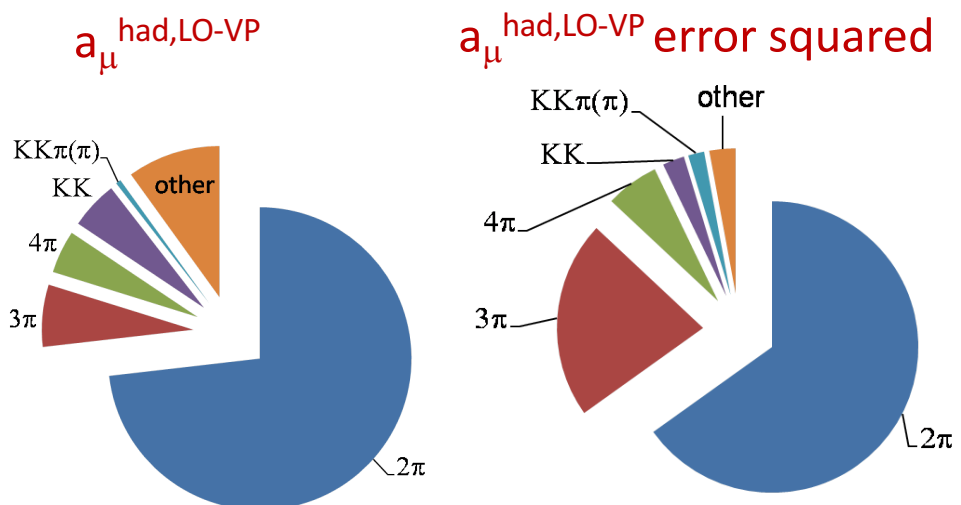
TABLE VII: Summary of the J/ψ and $\psi(2S)$ branching fractions.

Measured Quantity	Measured Value (eV)	J/ψ or $\psi(2S)$ Branching Fraction (10 ⁻³) Calculated, this work	PDG [28]
$\Gamma_{ee}^{J/\psi} \cdot \mathcal{B}_{J/\psi \rightarrow \pi^+\pi^-\pi^0\pi^0\pi^0}$	$35.8 \pm 4.4 \pm 5.4$	$6.5 \pm 0.8 \pm 1.0$	no entry
$\Gamma_{ee}^{J/\psi} \cdot \mathcal{B}_{J/\psi \rightarrow \eta\pi^+\pi^-\pi^0} \cdot \mathcal{B}_{\eta \rightarrow \pi^0\pi^0\pi^0}$	$21.1 \pm 1.7 \pm 3.2$	$11.9 \pm 0.9 \pm 2.3$	no entry
$\Gamma_{ee}^{J/\psi} \cdot \mathcal{B}_{J/\psi \rightarrow \omega\eta} \cdot \mathcal{B}_{\omega \rightarrow \pi^+\pi^-\pi^0} \cdot \mathcal{B}_{\eta \rightarrow \pi^0\pi^0\pi^0}$	$4.9 \pm 2.1 \pm 0.7$	$3.0 \pm 1.3 \pm 0.5$	1.74 ± 0.20
$\Gamma_{ee}^{J/\psi} \cdot \mathcal{B}_{J/\psi \rightarrow \omega\pi^0\pi^0\pi^0} \cdot \mathcal{B}_{\omega \rightarrow \pi^+\pi^-\pi^0}$	$9.4 \pm 2.3 \pm 1.5$	$1.9 \pm 0.5 \pm 0.3$	no entry
$\Gamma_{ee}^{J/\psi} \cdot \mathcal{B}_{J/\psi \rightarrow \pi^+\pi^-\pi^0\pi^0\eta} \cdot \mathcal{B}_{\eta \rightarrow \gamma\gamma}$	$10.6 \pm 1.6 \pm 1.6$	$4.9 \pm 0.8 \pm 0.8$	no entry
$\Gamma_{ee}^{\psi(2S)} \cdot \mathcal{B}_{\psi(2S) \rightarrow \pi^+\pi^-\pi^0\pi^0\pi^0}$	$3.3 \pm 2.3 \pm 0.5$	$1.4 \pm 1.0 \pm 0.2$	no entry
$\Gamma_{ee}^{\psi(2S)} \cdot \mathcal{B}_{\psi(2S) \rightarrow \eta\pi^+\pi^-\pi^0} \cdot \mathcal{B}_{\eta \rightarrow \pi^0\pi^0\pi^0}$	<3.0 at 90% C.L.	<3.5 at 90% C.L.	no entry
$\Gamma_{ee}^{\psi(2S)} \cdot \mathcal{B}_{\psi(2S) \rightarrow \omega\eta} \cdot \mathcal{B}_{\omega \rightarrow \pi^+\pi^-\pi^0} \cdot \mathcal{B}_{\eta \rightarrow \pi^0\pi^0\pi^0}$	<1.1 at 90% C.L.	<1.4 at 90% C.L.	<0.11 at 90% C.L.
$\Gamma_{ee}^{\psi(2S)} \cdot \mathcal{B}_{\psi(2S) \rightarrow \omega\pi^0\pi^0\pi^0} \cdot \mathcal{B}_{\omega \rightarrow \pi^+\pi^-\pi^0}$	<1.6 at 90% C.L.	<0.8 at 90% C.L.	no entry
$\Gamma_{ee}^{\psi(2S)} \cdot \mathcal{B}_{\psi(2S) \rightarrow \pi^+\pi^-\pi^0\pi^0\eta} \cdot \mathcal{B}_{\eta \rightarrow \gamma\gamma}$	<1.9 at 90% C.L.	<2.0 at 90% C.L.	no entry

New BaBar $e^+e^- \rightarrow \pi^+\pi^-\pi^0$

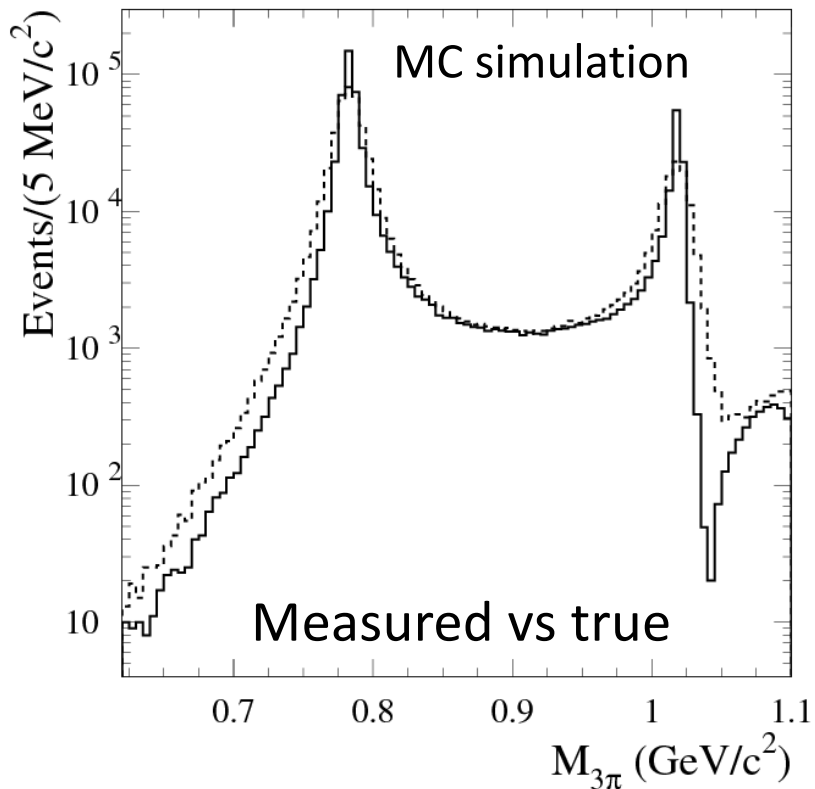
The process $e^+e^- \rightarrow \pi^+\pi^-\pi^0$ gives the second largest contribution into $a_\mu^{\text{had,LO-VP}}$ and its error.

Phys. Rev. D 70 (2004) 072004



- ✓ Previous BABAR measurement was based on 1/5 of the existing data set. The $e^+e^- \rightarrow \pi^+\pi^-\pi^0$ cross section was measured in the range 1.05-3 GeV – no XS below 1.05 GeV
 - ✓ In the new analysis we measure the cross section also below 1.05 GeV, in the region of the ρ , ω , and ϕ resonances.
 - ✓ Currently the $e^+e^- \rightarrow \pi^+\pi^-\pi^0$ contribution to $a_\mu^{\text{had,LO-VP}}$ is known with about 3% accuracy We plan to improve this accuracy to about 1.5%. Preliminary results ready for EPS2021(?)

$\pi^+\pi^-\pi^0$ mass spectrum below 1.1 GeV

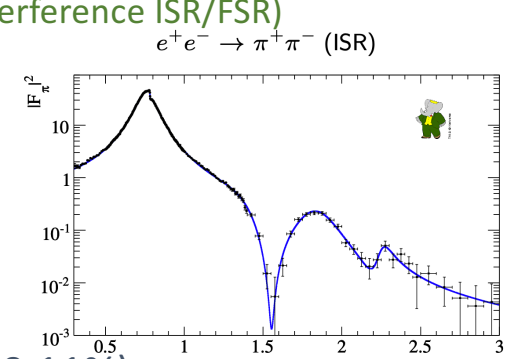


- The mass spectrum varies by 5 orders of magnitude and has narrow peaks. The result of unfolding strongly depends on quality of resolution simulation.
- To study data-MC difference in resolution, we fit to the observed mass spectrum with the VMD model.
- The widths of ω and ϕ resonances are measured with high accuracy. From the fit we determine parameters of the (narrow) Gaussian smearing function.
- The long tails of the mass resolution function depend on requirement on χ^2 of the kinematic fit used for event selection. To understand quality of the tail simulation, we compare results of the VMD fit for spectra obtained with different cuts on χ^2 .

New BABAR ISR $\mu\mu\gamma$ / $\pi\pi\gamma$ / $KK\gamma$ analysis

Published analysis : PRL 2009 ($\pi\pi/\mu\mu$) + PR 2012 ($\pi\pi/\mu\mu$) + PR 2014 ($K+K-$) + PR 2014 (interference ISR/FSR)

- PID used to separate $\pi\pi\gamma$ and $\mu\mu\gamma$ channels
- $P>1$ GeV to ensure reliable μ ID
- NLO kinematic fits (2 charged tracks + main ISR γ + add ISR or FSR γ)
- Runs 1-4 (half statistics)
- Trigger, tracking, PID efficiencies obtained by the tag&probe method
- For $\pi\pi\gamma/\mu\mu\gamma$ ratio: **PID systematic uncertainty dominant (0.44%)**, tracking (0.11%)
- NLO kinematic fits with loose χ^2 cuts to ensure low inefficiency

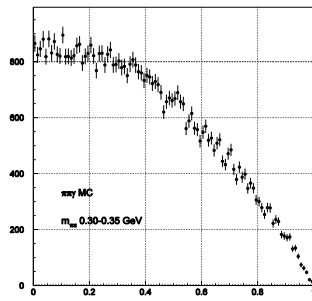


New analysis in progress → 2022

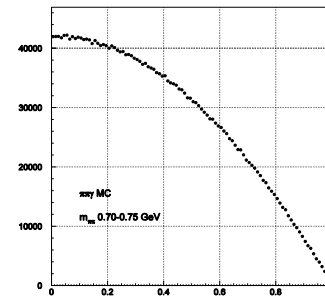
- $\pi\pi\gamma$, $KK\gamma$, and $\mu\mu\gamma$ samples separated by fitting the angular distribution in the 2-particle CM: essential to keep low-momentum tracks
- Trigger and tracking efficiency method needs to be extended for tracks well below 1 GeV
- In practice tracks are reconstructed in BABAR down to $p_T \sim 0.1$ GeV/c
- Runs 1-6 (full data + no PID ⇒ **statistics ×7 and smaller systematic uncertainty, blind**)
- Improved NLO kinematic fits + NNLO fits for checks
- Mass range limited to ~1.4 GeV (>99% of $\pi\pi$ contribution to a_μ)

MC angular distributions ($|\cos \theta^*_\pi|$)

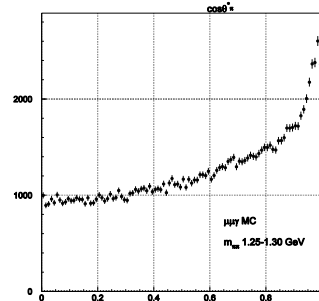
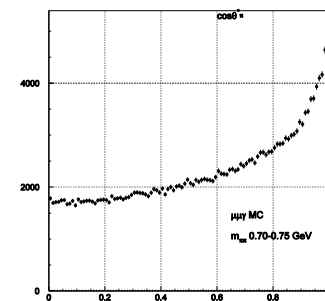
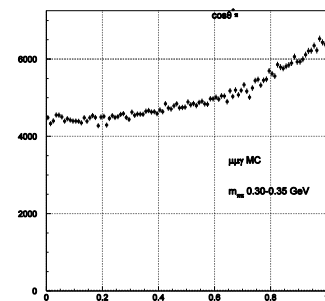
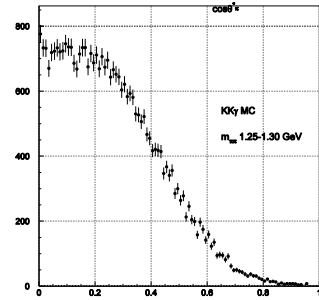
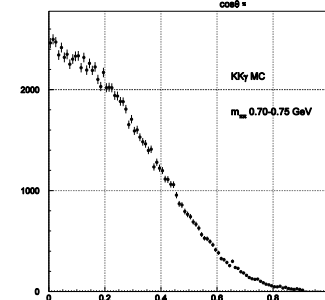
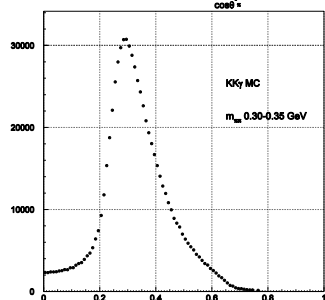
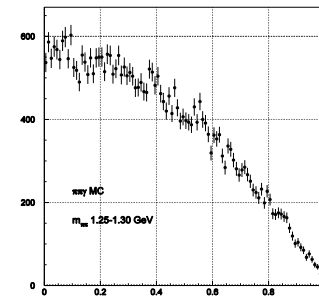
$m_{\pi\pi}$ (GeV) 0.30-0.35



0.70-0.75



1.25-1.30



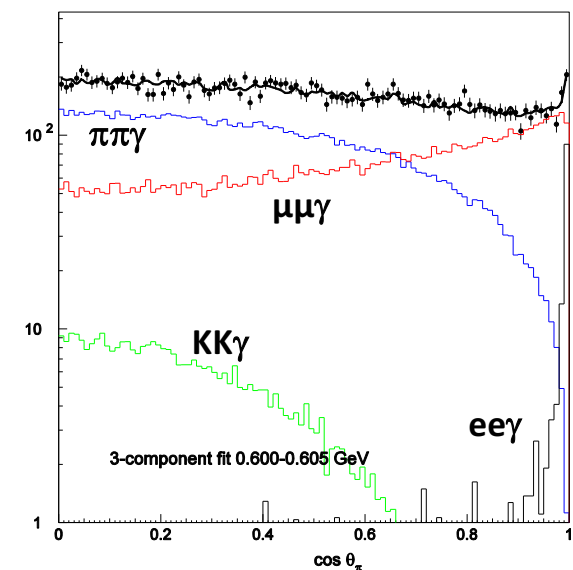
29.06.2021

Solodov BaBar

$\pi\pi\gamma$

preliminary fits (test sample)

$KK\gamma$



$\mu\mu\gamma$

22

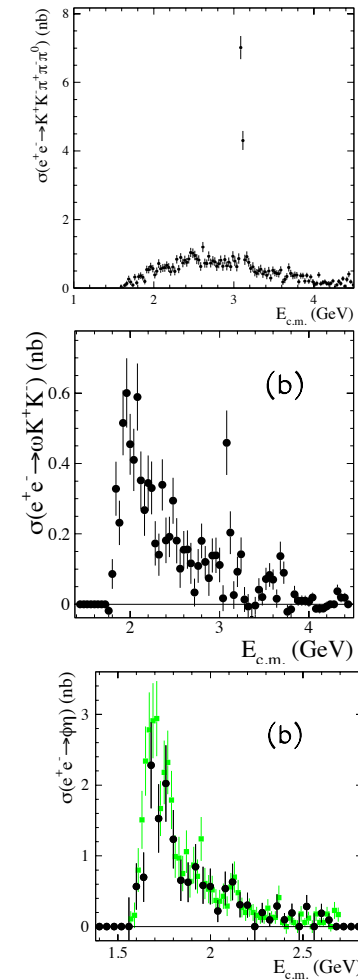
New: $2K3\pi$

Below 2 GeV, probably, (last?) final state with sizable XS,
which is included(?) via iso-spin relations, is $e^+e^- \rightarrow K\bar{K}3\pi$

What we know:

- 1. $e^+e^- \rightarrow K^+K^-\pi^+\pi^-\pi^0$ - the only measured XS – BaBar
Phys.Rev. D76 (2007) 092005
- 2. $e^+e^- \rightarrow K^+K^-\pi^0\pi^0\pi^0$ - No info . Partly from $\phi\eta$
- 3. $e^+e^- \rightarrow K_S K_L \pi^0\pi^0\pi^0$
 $e^+e^- \rightarrow K_S K_L \pi^+\pi^-\pi^0$
 $e^+e^- \rightarrow K_S K_S \pi^+\pi^-\pi^0$
- 4. $e^+e^- \rightarrow K^+K_{S,L}\pi^+\pi^0\pi^0$ - No info
- 5. $e^+e^- \rightarrow K^+K_{S,L}\pi^+\pi^+\pi^-$ - No info

Analysis is in progress



Conclusion

- BaBar is continuing to present data for the low energy e^+e^- cross sections
- Results for two new analyses of multi-hadron processes are presented
- Most important for g-2 analyses ($e^+e^- \rightarrow \pi^+\pi^-$, $\pi^+\pi^-\pi^0$) are revisiting using full data set
- If no ideas, these two and $2K3\pi$ studies will move this BaBar program to the end (?)

Thank you